JCB Article

The endoplasmic reticulum cation P-type ATPase Cta4p is required for control of cell shape and microtubule dynamics

Anna L. Okorokova Façanha,[1] Henrik Appelgren,[2] Mohammad Tabish,[2] Lev Okorokov,[1] and Karl Ekwall[2]

[1]Laboratório Fisiologia e Bioquímica de Microrganismos, Centro de Biociências e Biotecnologia, Universidade Estadual do Norte Fluminense, Campos dos Goytacazes, Horto, CEP 28015-620, Brazil
[2]Karolinska Institutet, Department of Biosciences Novum/University College Sodertorn, Deptartment of Natural Sciences, S-141 04 Huddinge, Sweden

Here we describe the phenotypic characterization of the *cta4*$^+$ gene, encoding a novel member of the P4 family of P-type ATPases of fission yeast. The *cta4Δ* mutant is temperature sensitive and cold sensitive lethal and displays several morphological defects in cell polarity and cytokinesis. Microtubules are generally destabilized in cells lacking Cta4p. The microtubule length is decreased, and the number of microtubules per cell is increased. This is concomitant with an increase in the number of microtubule catastrophe events in the midzone of the cell. These defects are likely due to a general imbalance in cation homeostasis. Immunofluorescence microscopy and membrane fractionation experiments revealed that green fluorescent protein–tagged Cta4 localizes to the ER. Fluorescence resonance energy transfer experiments in living cells using the yellow cameleon indicator for Ca^{2+} indicated that Cta4p regulates the cellular Ca^{2+} concentration. Thus, our results reveal a link between cation homeostasis and the control of cell shape, microtubule dynamics, and cytokinesis, and appoint Ca^{2+} as a key ion in controlling these processes.

Introduction

The P-type ATPases are present in all living cells where they mediate ion transport across membranes on the expense of ATP hydrolysis. Among the ions transported by these pumps are protons, calcium, sodium, potassium, and heavy metals such as manganese, iron, copper, and zinc. The formation of a phosphorylated intermediate during the catalytic cycle is a characteristic of P-type ATPases that distinguishes them from V ATPases and F ATPases (Pedersen and Carafoli, 1987a,b).

Within the protein family of P-type ATPases, the Ca^{2+}-ATPases are of special interest, since calcium plays a key role in signal transduction in eukaryotic cells (Clapham, 1995). The transient elevation in cytosolic-free calcium stimulates several Ca^{2+}-binding proteins and their targets that act to elicit downstream signaling pathways. Ubiquitous effectors of calcium signaling are Ca^{2+}/calmodulin (CaM)*-dependent protein kinases and Ca^{2+}/CaM-dependent phosphatase, calcineurin, which act by modulating the phosphorylation state of diverse proteins including transcription factors (Stull, 2001). There is a growing body of evidence that the cellular response to a rise in calcium depends on the amplitude, frequency, duration, and location of the Ca^{2+} signal (Sanders et al., 1999). The calcium signal is terminated when cytosolic-free Ca^{2+} concentration is reduced to basal levels by Ca^{2+}-ATPases and Ca^{2+}/H^+ exchangers that transport calcium from the cell or sequester it in organelles. In the last case, refilling of intracellular compartments safeguards the Ca^{2+} release during subsequent signaling events and provides a lumenal space with specific Ca^{2+} concentration required for diverse biochemical reactions taking place in those compartments (Corbett and Michalak, 2000).

Two main classes of Ca^{2+}-ATPases have been described: sarco/ER Ca^{2+}-ATPases (SERCA) and plasma membrane Ca^{2+}-ATPases, which differ from one another in their subcellular distribution, biochemical characteristics, and mode of regulation (Guerini and Carafoli, 1999; Carafoli and Brini, 2000). In addition, the secretory pathway Ca^{2+}-ATPases initially characterized in budding yeast (Rudolph

Address correspondence to Karl Ekwall, University College Sodertorn, Dept. of Natural Sciences, Alfred Nobels Alle 3, S-141 52 Huddinge, Sweden. Tel.: 46-8-608-4713. Fax: 46-8-608-4510. E-mail: karl.ekwall@cbt.ki.se

*Abbreviations used in this paper: CaM, calmodulin; CoA, coenzyme A; CsA, cyclosporin A; CYP, cyan fluorescent protein; FRET, fluorescence resonance energy transfer; GFP, green fluorescent protein; IF, immunofluorescence; SERCA, sarco/ER Ca^{2+}-ATPases; TBZ, thiabendazole; TMD, transmembrane spanning domain; YFP, yellow fluorescent protein.

Key words: *Schizosaccharomyces pombe*; P-type ATPase; endoplasmic reticulum; calcium; microtubule

Table I. **Cta4 ATPase belongs to the P4 family of P-type ATPases**

P-type consensus[a]	Cta4 sequence	Putative function in Cta4
LTGES	$_{307}$LSGES$_{311}$	Unknown
$^{F}/_{S}$DKTGTLT	$_{484}$FDKTGTLT$_{491}$	Phosphorylation site
KGA--	$_{614}$KGAPE$_{618}$	ATP binding
M•TGD	$_{706}$MITGD$_{710}$	ATP binding
GDG•ND	$_{823}$CGDTND$_{828}$	Coupling ATP-binding domain to domain involved in ion transport

Underline denotes conservative replacement, indicated by • in the consensus.
[a]Catty et al., 1997.

et al., 1989) has emerged as a separate class (Gunteski-Hamblin et al., 1992; Sorin et al., 1997).

The fission yeast *Schizosaccharomyces pombe* is an excellent model system for eukaryotic cell biology. Several components of Ca^{2+}-mediated signaling of animal cells have been identified and characterized in fission yeast. A temperature-sensitive Ca^{2+}-binding site CaM mutant exhibits broken spindles and defects in chromosome segregation (Moser et al., 1997). CaM is localized to the spindle pole bodies and sites of polarized cell growth in *S. pombe* (Moser et al., 1997). In cells undergoing cytokinesis, CaM was found on both sides of septum. Similar CaM redistribution at the cell equator was observed in dividing animal cells where CaM activation by elevation of free Ca^{2+} was proposed to trigger the formation of the cleavage furrow (Li et al., 1999). Thus, there are several indications that Ca^{2+} and CaM have an important role in regulating aspects of the cytokinesis both in animal cells and fission yeast, but more direct evidence for Ca^{2+} affecting this process is lacking.

Recently, the gene *ppb1*$^{+}$ encoding for the catalytic subunit of calcineurin was isolated from *S. pombe* (Yoshida et al., 1994; Plochocka-Zulinska et al., 1995). Mating, microtubule distribution, chromosome segregation, spindle pole body, and nuclear positioning were impaired in calcineurin-deficient cells (Yoshida et al., 1994). The lack of *ppb1*$^{+}$ resulted in branched cells with multiple septa that fail to cleave. These observations further indicate that Ca^{2+} homeostasis can have profound effects on cytoskeleton functions in fission yeast.

In spite of these findings, little is known about how calcium signals are generated and controlled in *S. pombe*, and so far little is known about the molecular identity of transporters, which deplete cytosolic calcium. The *cta3*$^{+}$ gene product was identified previously as a Ca^{2+}-ATPase (Ghislain et al., 1990) and is related to the ENA1 Na^{+}-ATPase of *Saccharomyces cerevisiae*. Cta3p is required for Na^{+} tolerance in *S. pombe* (Nishikawa et al., 1999). The Ca^{2+}/H^{+} exchangers were shown to be responsible for Ca^{2+} transport in membranes of the secretory pathway organelles, but Ca^{2+}-ATPase activity has so far not been detected in membrane preparations (Okorokov et al., 2001). Although the genes encoding for several putative calcium ATPases were identified by the *S. pombe* genome-sequencing project, no genetic analysis has been performed on the corresponding null mutants. Thus, the involvement of each individual pump in calcium homeostasis and the role of the pumps in signal transduction and diverse cellular functions have not been established. Toward this end, we have here determined the subcellular localization of the putative calcium ATPase SPAC2E11.07C and analyzed the physiological consequences of its gene deletion. To follow the preexisting nomenclature of P-type ATPases in fission yeast, SPAC2E11.07C was named *cta4*$^{+}$ (calcium/cation transporting ATPase). The *cta4*$^{+}$ gene encodes a novel member of the P4 family of P-type ATPases that is localized in the ER. *cta4*$^{+}$ is not an essential gene, but *cta4Δ* mutants display several morphological defects, an imbalance in cation homeostasis and are temperature sensitive and cold sensitive lethal. Microtubules are generally destabilized in cells lacking Cta4p. The microtubule length is decreased, and the number of microtubules per cell is increased concomitant with an increase in the number of microtubule catastrophe events in the midzone of the cell. Fluorescence resonance energy transfer (FRET) experiments in living cells using the fluorescent yellow cameleon indicator for Ca^{2+} indicated that a deletion of *cta4*$^{+}$ causes an elevation of cellular calcium levels. Our results reveal a link between control of cell shape, microtubule dynamics, cytokinesis, and cation homeostasis, and appoint Ca^{2+} as a key regulatory ion. Hence, our data points to a new level of control over these important processes.

Results

Analysis of the *cta4*$^{+}$ gene

The full-length SPAC2E11.07C gene (sequence data available from GenBank/EMBL/DDBJ under accession no. O14072) referred to here as *cta4*$^{+}$ encodes a 1211–amino acid–long protein. Twelve transmembrane spanning domains (TMDs) and three defined hydrophilic cytosolic domains linking TMDs 2 and 3, 4 and 5, and 6 and 7 were predicted by topological analysis. Sequence analysis indicates that

Table II. **Identification of P4-ATPase signatures in Cta4**

P4-ATPases signatures[a]	Cta4 sequence
$^{D}_{L}$I•T--•PP$^{A}_{E}$LP	$_{435}$M**II**TSV**V**P**S**E**LP**$_{446}$
$^{M}_{F}$C***•**$^{C}_{V}$	$_{821}$M**C**GDG**T**ND**V**$_{829}$
••S-$^{A}_{C}$•$^{P}_{S}$FTS$^{K}_{N}$---•--•--••-$^{E}_{Q}$GR$^{C}_{A}$•LV$^{T}_{N}$•	$_{959}$D**A**S**A**A**P**F**TSK**LAV**V**SS**I**TN**IV**R**QGRCTLV**AL$_{990}$

Underline denotes conservative replacement, indicated by • in the consensus. Bold denotes conserved amino acids in the P4-ATPase specific sequences. Highly conserved amino acids in P-type ATPases are indicated by * in the consensus.
[a]Catty et al., 1997.

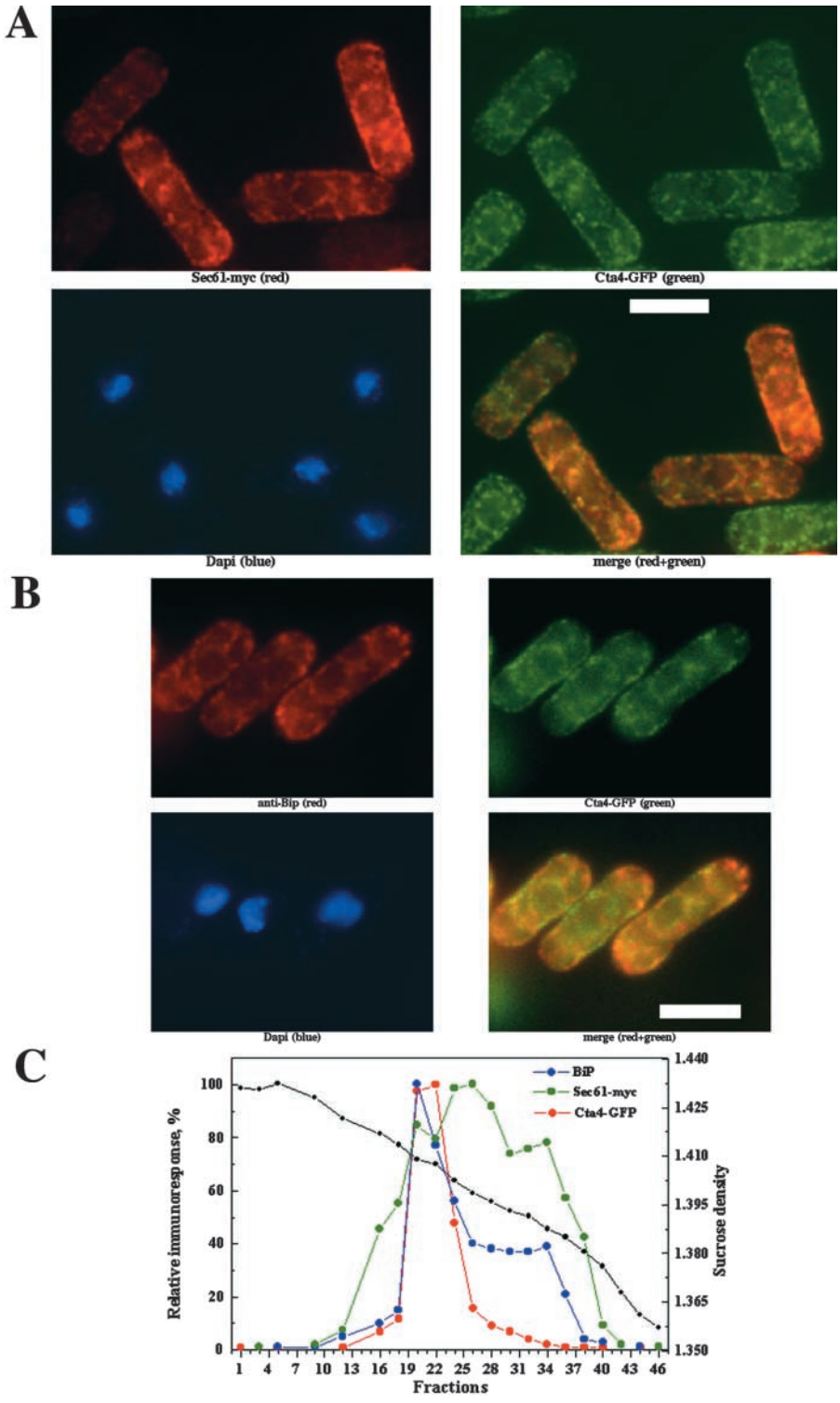

Figure 1. **Cellular localization of Cta4p.** (A and B) Yeast cells were grown to early log phase, fixed and stained with antibodies, and examined by IF microscopy (as described in Materials and methods). (A) GFP-tagged Cta4p cells transformed with plasmid-encoding Sec61-myc fusion protein (Broughton et al., 1997) were subjected to IF and stained with anti-GFP (green), anti-myc (red), and DAPI (blue). The cell to cell variation in expression of Sec61-myc is due to unequal partitioning of the multicopy plasmid. Bar, 10 μm. (B) Wild-type cells expressing GFP-tagged Cta4p stained with anti-GFP (green), anti-BiP (red), and DAPI (blue). The merged images show colocalization of Cta4p with Sec61 and BiP (yellow) in the deconvolved image. (C) Cta4p is comigrating with ER membranes. Total membranes were isolated from the cells expressing both Cta4-GFP and Sec61-myc fusion proteins, fractionated on a sucrose density gradient, and submitted to immunoblot analysis. Dot blots of individual fractions were used for quantification of the relative levels of Cta4, Sec61, and BiP in membrane fractions. A fraction with higher immunoresponse was considered as 100% in each case.

Cta4p has all five highly conserved domains characteristic of ion transporting P-type ATPases (Tables I and II). These include the potential phosphorylation site represented by Asp^{485} and the domains involved in ATP binding, all located in a large hydrophilic loop between TMDs 6 and 7. Search for homologues in the GenBank database revealed that Cta4p is related to the *S. cerevisiae* ORF Yel031p, which encodes the Spf1 ATPase that belongs to the family of P4-ATPases with unknown substrate specificity (Catty et al., 1997). The Cta4p sequence shares specific amino acid sequence motifs intrinsic for P4 ATPases with the Spf1 amino acid sequence. These include one Cys residue preceding the consensus motif GDG×ND and the ××S4×FTS14×GR××LV×× sequence (Tables I and II). Whereas the highest sequence identity was obtained with the *SPF1* gene product in amino acid sequence comparisons (49% overall identity), other *S. cerevisiae* cation ATPases, such as Na^+-ATPase ENA1 and Ca^{2+}-ATPases PMR1 and PMC1, showed a relatively low sequence similarity with Cta4p (14.2, 15.1, and 12.6% overall amino acid identities, respectively). The Cta4p sequence showed low

overall identity (13.7%) with Cta3p of *S. pombe* (Ghislain et al., 1990). Besides *SPF1* of *S. cerevisiae*, human KIAA1825 protein expressed in brain (sequence data available from GenBank/EMBL/DDBJ under accession no. AB058728) (Nagase et al., 2001) had a high sequence similarity to Cta4p (37.7% overall amino acid identity).

Cta4-GFP is localized to the ER

To investigate the intracellular localization of the Cta4 ATPase in fission yeast, a fusion protein between Cta4p at its COOH terminus and the green fluorescent protein (GFP) was generated (see Materials and methods). The Cta4-GFP gave a weak signal in live cells, but the fusion protein was readily detected by indirect immunofluorescence (IF) microscopy using antibodies against GFP (Fig. 1 A). The Cta4-GFP fusion protein is replacing the endogenous *cta4*$^+$ allele and is thus expressed from the natural *cta4*$^+$ promoter and is fully functional (see below). The localization pattern of the Cta4-GFP was found to be similar to that of Sec61, a known ER marker (Broughton et al., 1997) as revealed by IF. To test for colocalization of these two proteins, Sec61 fused to the c-myc epitope tag was expressed from a plasmid in the strain carrying Cta4-GFP (Fig. 1 A). Digital confocal microscopy revealed a partial colocalization of both proteins, suggesting that the Cta4 ATPase at least in part resides in the ER.

These data were further confirmed by subcellular fractionation of total membranes isolated from cells expressing both Cta4-GFP and Sec61-myc fusion proteins. Immunoblots of membrane fractions showed that Cta4-GFP comigrated with Sec61-myc at positions within the gradient corresponding to 41–47% sucrose where membrane vesicles enriched with ER were shown previously to migrate (Fig. 1 C) (Okorokov et al., 2001). However the Sec61-myc fusion protein showed a wider distribution than Cta4-GFP and was also detected in membrane fractions migrating at 32–41% sucrose corresponding to the Golgi and/or Golgi-like membranes. Thus, it is likely that this broader distribution of Sec61-myc corresponds to Golgi and that Cta4-GFP is more restricted to the ER. In animal cells, a Sec61 homologue was found in the ER-to-Golgi intermediate compartment in addition to the ER, thus supporting this idea (Greenfield and High, 1999; Kamhi-Nesher et al., 2001). Another possible explanation for the broader distribution of Sec61-myc might be its overexpression from a plasmid.

To verify the ER localization of Cta4 ATPase, the antibody against another ER organelle marker, chaperone BiP (Pidoux and Armstrong, 1993), was used. IF microscopy demonstrated colocalization of Cta4-GFP and BiP (Fig. 1 B). Distribution of BiP in membrane fractions was more restricted than that of Sec61-myc and was similar to that of Cta4. Both BiP and Cta4 proteins were concentrated in fractions 20–22 (Fig. 1 C). Therefore, it could be concluded from these results that Cta4 ATPase is localized to the ER compartment.

cta4$^+$ regulates cation homeostasis

To further investigate the function of Cta4p in fission yeast, the *cta4*$^+$ gene was disrupted with the *ura4*$^+$ marker gene, and the resulting *cta4Δ* phenotype was compared with that of wild type. Tetrad analysis revealed that *cta4*$^+$ was not an essential gene; however, *cta4Δ* cells exhibited poor growth at 25°C compared with that at 30°C and died at 36°C, indicating that some

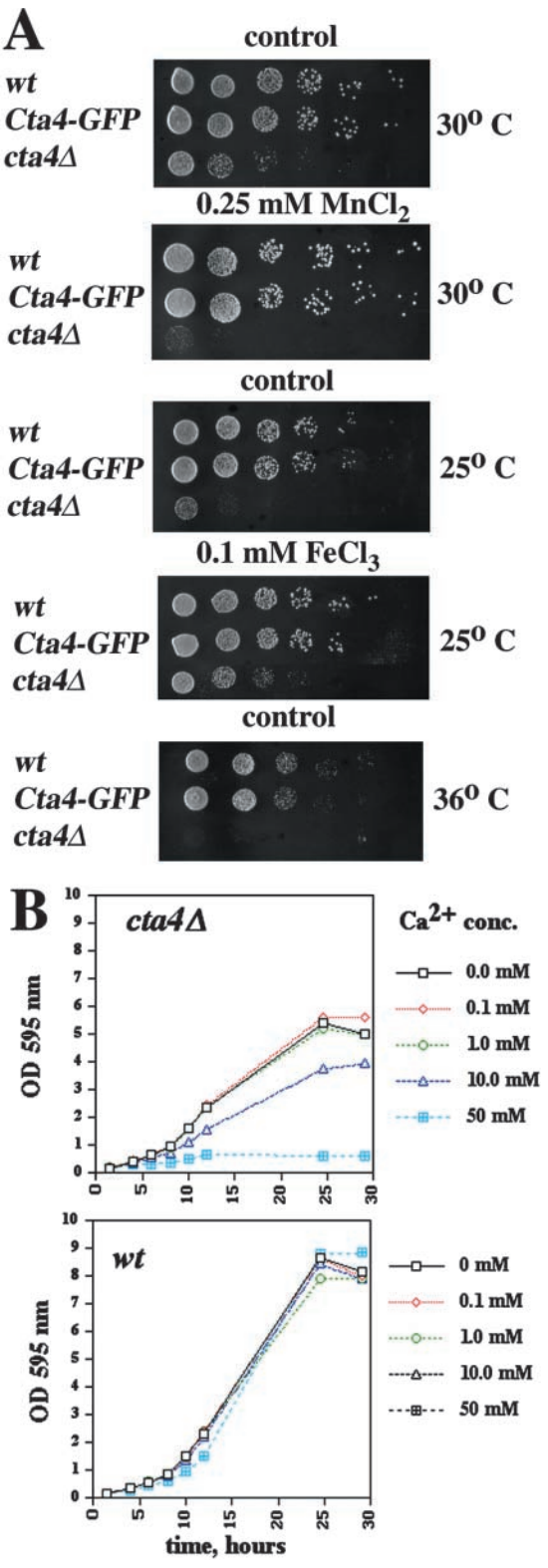

Figure 2. **Phenotypes of *cta4Δ*.** (A) Disruption of *cta4*$^+$ confers a temperature-sensitive phenotype and causes an imbalance in cation homeostasis. Cells were serially diluted in fivefold steps, spotted onto YES plates containing cations as indicated, and incubated for 3 d at 25, 30, or 36°C. Strains used were Fy1180, Hu185, and Hu285. (B) The effect of Ca^{2+} on the growth of the *cta4Δ* mutant. Growth curves showing the growth inhibition by different concentrations of $CaCl_2$ at 30°C.

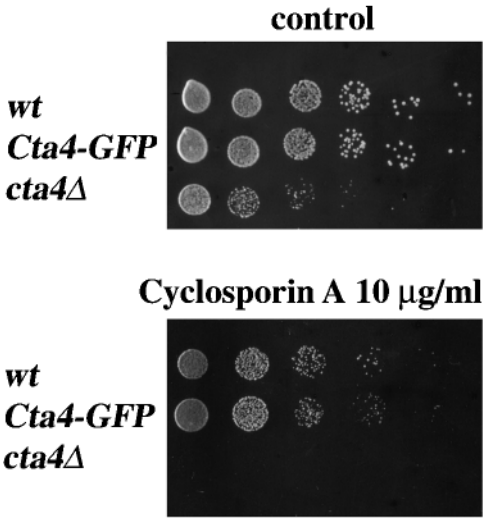

Figure 3. **Viability of *cta4Δ* depends on calcineurin.** Cells were serially diluted in fivefold steps, spotted onto YES plates containing 10 μg/ml CoA, and incubated for 3 d at 30°C. Strains used were Fy1180, Hu185, and Hu285.

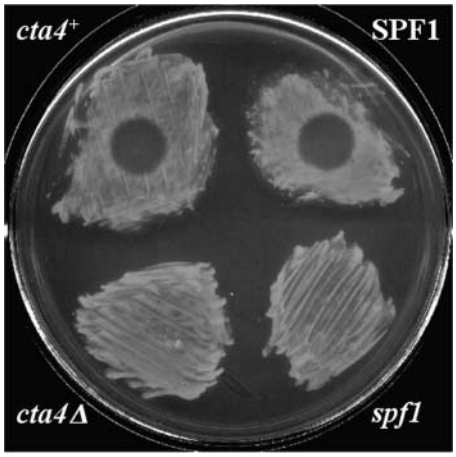

Figure 4. **Loss of *cta4*$^+$ confers a resistance to *P. farinosa* killer toxin SMKT.** The wild-type (Fy1180) and *cta4* mutant cells (Hu285) were spread on the MB plates on which 5 μl of 100 μM SMKT solution was spotted (arrowhead). The *S. cerevisiae* strains used were CS202A and CS202B.

aspect of cell cycle progression was impaired in these conditions (Fig. 2 A). Growth of Cta4-GFP cells was not impaired at 25 and 36°C, pointing out that this allele is fully functional.

Yeast P-type ATPase mutants commonly display phenotypic defects in response to variations in the concentration of cations in the growth media (Rudolph et al., 1989; Cunningham and Fink, 1996). Consistent with this idea, we found that growth of *cta4Δ* cells was completely inhibited by a high concentration, that is, 100 mM of $CaCl_2$. Next, growth inhibition of lower concentrations of $CaCl_2$ was investigated using liquid cultures (Fig. 2 B). It was clear that the growth of wild-type cells was unaffected by addition of up to 50 mM $CaCl_2$, whereas the growth of *cta4Δ* cells was partially inhibited already by the addition of 10 mM $CaCl_2$ and completely inhibited by the addition of 50 mM $CaCl_2$. The *cta4*$^+$ deletion mutant was also sensitive to 0.25 mM $MnCl_2$ (Fig. 2 A). Furthermore, the *cta4Δ* growth at 25°C was improved by high concentrations of Fe^{3+} (0.1 mM $FeCl_3$) (Fig. 2 A), and the lethality of *cta4Δ* at 36°C could be overcome by K^+ (300 mM KCl), ruling out that Cl^- could be toxic to *cta4Δ* cells (unpublished data). Collectively, these results showed that the homeostasis of different ions is severely compromised in *cta4Δ* cells. Although the data did not elucidate which cation is transported by the *cta4*$^+$ gene product, they strongly suggest that Cta4 ATPase might have a crucial function in maintenance of cation homeostasis in fission yeast. This conclusion was further reinforced by the observation that overexpression of *cta4*$^+$ from the regulatable *nmt1*$^+$ promoter was deleterious to wild-type cells, but growth was restored by the addition of 100–200 mM $CaCl_2$ (unpublished data).

The Ca^{2+}/CaM-dependent protein phosphatase 2B, calcineurin, was shown to be responsible for a maintenance of cation homeostasis in *S. cerevisiae* by regulating the expression of Ca^{2+} and Na^+ ATPases (Nakamura et al., 1993; Cunningham and Fink, 1996; Mendoza et al., 1996). In *S. pombe*, the calcineurin A subunit-like protein encoded by the *ppb1*$^+$ gene is the target of cyclosporin A (CsA) (Yoshida et al., 1994). *cta4Δ* cells were found to be susceptible to 10 μg/ml CsA (Fig. 3), whereas wild-type strain remained insensitive to threefold higher drug concentration. This result indicates that *cta4*$^+$ acts in the same or parallel pathways as calcineurin, since *ppb1*$^+$ seems necessary for the viability of the *cta4Δ* mutant.

Functional similarity with the *S. cerevisiae* Spf1 ATPase

Because Cta4 ATPase shares 49% homology with *S. cerevisiae* Spf1p whose deletion confers resistance to *Pichia farinosa* killer toxin, SMKT (Suzuki and Shimma, 1999), we investigated the effect of SMKT on fission yeast wild-type and *cta4Δ* cells. In the halo assay, the wild-type strain displayed a clear sensitivity to SMKT, whereas *cta4Δ* was resistant to the toxin (Fig. 4). It was proposed that the resistance to killer toxin in *spf1* null might be due to an alteration in glycosylation of the cell wall components (Suzuki and Shimma, 1999). The enzymes involved in the glycosylation process require Mn^{2+} for their activity (Kaufman et al., 1994). Therefore, the resistance to SMKT displayed by *cta4Δ* cells is not surprising, since the *cta4Δ* mutant also exhibits defects in Mn^{2+} homeostasis (Fig. 2 A). Thus, both Spf1 and Cta4 could have similar functions both with respect to Mn^{2+} homeostasis and the response to SMKT. It has been shown recently that SMKT interacts with the plasma membrane of wild-type but not mutant *spf1* cells (Suzuki et al., 2001), raising a possibility that a structure and/or targeting of some membrane component, which binds the toxin, is similarly affected in *S. cerevisiae spf1* and *S. pombe cta4* mutant cells.

cta4$^+$ is required for cytokinesis and microtubule integrity

Next, the effect of *cta4*$^+$ gene disruption on cell morphology was investigated. *cta4Δ* cells were frequently multiseptated and formed hyphae-like structures, in which cells were not separated even when grown at the permissive temperature of 30°C. These multicellular structures were often branched and aggregated (Fig. 5 A). Lowering or increasing the temperature from 30°C or adding $CaCl_2$ to the cells aggravated the phenotype. The multiseptated phenotype suggested that Cta4p is required for the final stages of cytokinesis. The aberrant cell shapes exhibited by *cta4Δ* also suggested that the cells had defects in the cytoskeleton. To test if microtubule function was

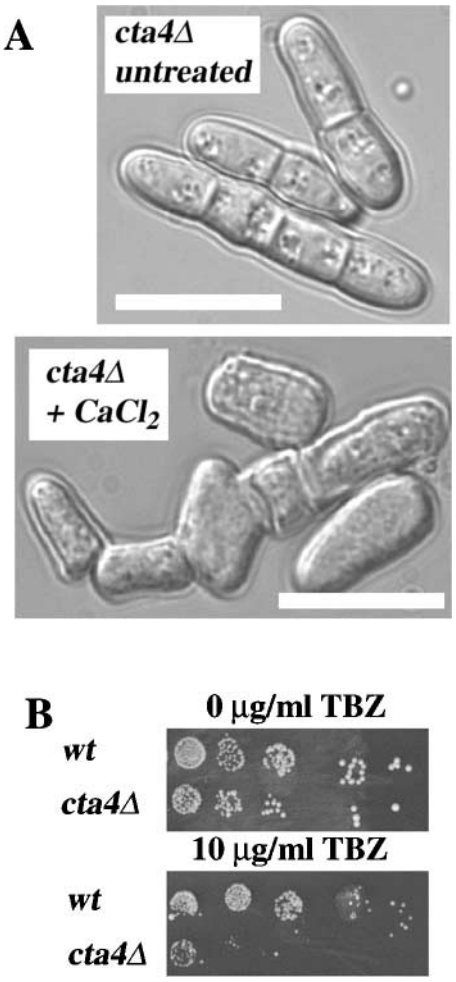

Figure 5. **Cell shape defects, cytokinesis defects, and TBZ sensitivity of the *cta4Δ* mutant.** (A) Aberrant cell morphology of *cta4Δ* cells. Phase–contrast micrographs of *S. pombe* wild-type and *cta4Δ* cells grown in YES medium at 30°C. Bars, 10 μm. (B) TBZ sensitivity of *cta4Δ*. Strains grown at 30°C were 972 and Hu285.

perturbed in *cta4Δ* cells, growth in the presence of the microtubule destabilizing drug thiabendazole (TBZ) was assayed. *cta4Δ* cells were found to be sensitive to TBZ, indicating that Cta4p is normally required to stabilize microtubules (Fig. 5 B). To examine whether loss of $cta4^{+}$ leads to changes in microtubule assembly, microtubules in *cta4Δ* cells were visualized using monoclonal antitubulin antibodies by IF microscopy of cells grown at 25°C. Cytoplasmic microtubules in the mutant cells appeared abnormally short, and the number of microtubules per cell was increased in *cta4Δ* cells compared with wild-type cells (Fig. 6, A and B). Measurements of the microtubule length indicated that the microtubules in interphase *cta4Δ* cells were significantly shorter ($t = -3.573$; $P = 0.001$) than those of wild-type cells. The microtubules in *cta4Δ* cells rarely reached lengths greater than 4 μm, whereas those of wild-type cells extended up to 8 μm (Fig. 6 C). Furthermore, the number of microtubules per interphase cell was markedly increased in *cta4Δ* cells to three to six microtubules per cell, whereas wild-type cells had only one to three (Fig. 6 D). Thus, Cta4p generally stabilizes microtubules.

To test if the shortening and increase in microtubule number per cell were due to altered dynamic properties of the

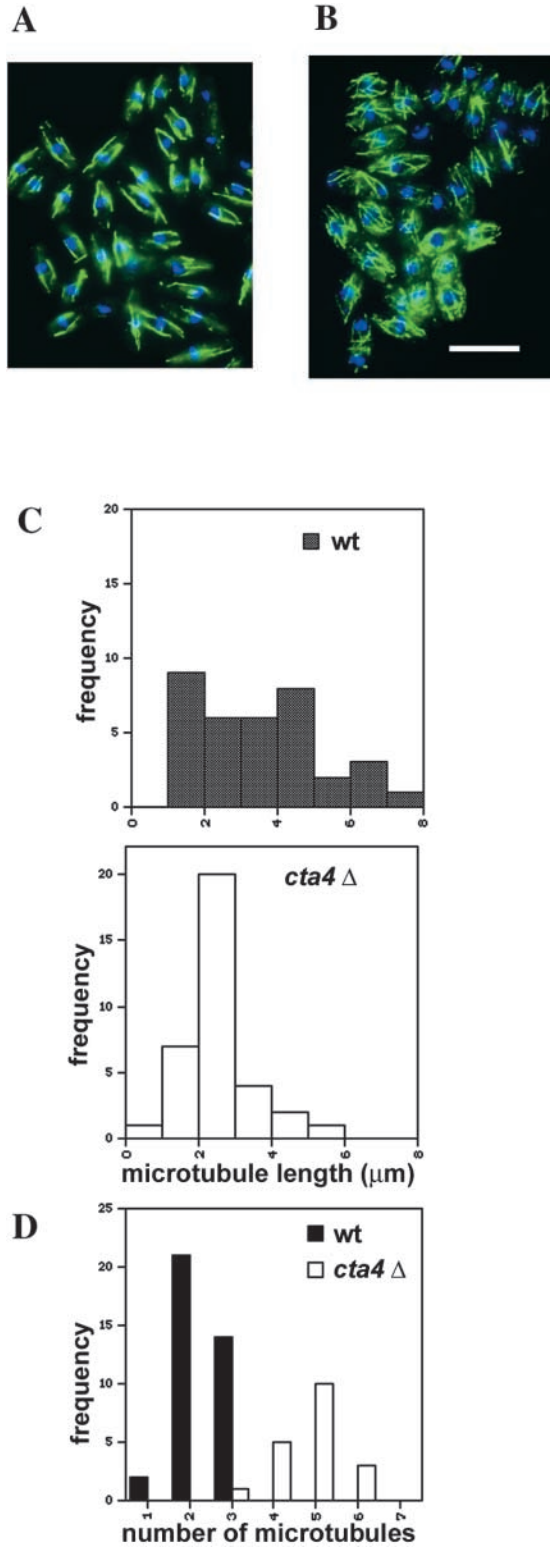

Figure 6. **Microtubule distribution in *cta4Δ* cells.** (A and B) IF microscopy images of wild-type (A) and *cta4Δ* cells (B) grown at 25°C and fixed and stained with anti-TAT1 (green) and DAPI (blue). Bar, 10 μm. (C) Analysis of microtubule length (*cta4Δ*, $n = 47$; wt, $n = 35$) (D) Analysis of the number of microtubules per interphase cell (*cta4Δ*, $n = 47$; wt, $n = 35$).

microtubules, we investigated the microtubule dynamics in living wild-type and *cta4Δ* cells using strains expressing α-tubulin fused to GFP (Ding et al., 1998; Pidoux et al., 2000). The

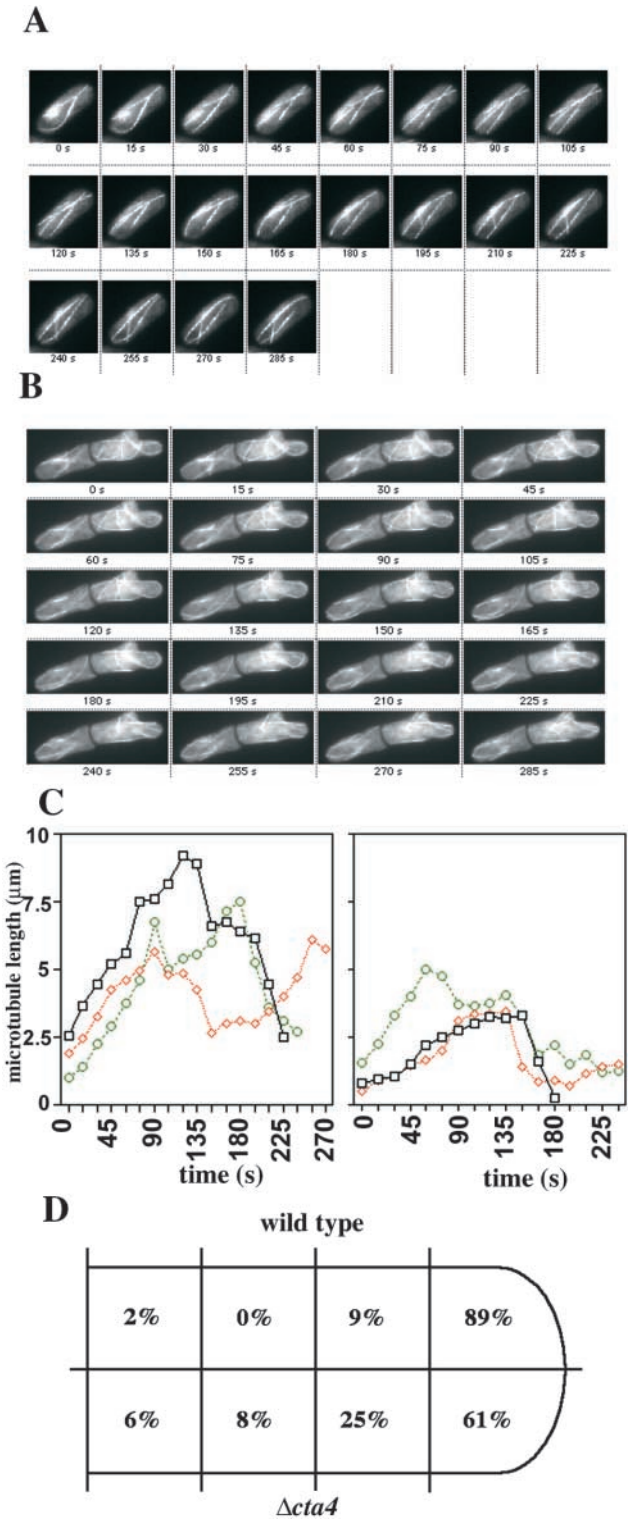

Figure 7. **Microtubule dynamics are altered in *cta4Δ* cells.** (A) A time-lapse series of images of wild-type cells expressing GFP-tagged α-tubulin. (B) A time-lapse series of *cta4Δ* cells expressing GFP-tagged α-tubulin. (C) Growth of individual microtubules in wild-type (left) and *cta4Δ* (right) cells. (D) The schematic drawing is representing the frequencies of catastrophe event in different parts of the cell. Strains used were Fy2773 and Hu326.

analysis of time-lapse movies of α-tubulin–GFP fusion confirmed the alterations observed in fixed cells, namely that the number of microtubules per cell was markedly increased in cells lacking Cta4p (Fig. 7, A and B). In addition, cells lacking *cta4*$^+$ exhibited changes in the microtubule growth rate and in the occurrence of microtubule catastrophe events. Length measurements of individual microtubules revealed that, although the microtubules of wild-type cells commonly reached a length of >5 μm before they suddenly started to shrink, those of *cta4Δ* cells underwent catastrophe events already at lengths of ~3 μm (Fig. 7 C). Moreover, the microtubule catastrophe events in *cta4Δ* cells were not limited to a cortical region near the cell tip, whereas those in wild-type cells in 89% of the cases occurred in the cell tip region (Fig. 7 D). Thus, the time-lapse analysis revealed that the dynamic features of microtubules were strongly altered in *cta4Δ* cells, leading to a failure in guiding the microtubules toward the cell tip so that the cell growth axis could not be maintained.

cta4$^+$ controls the nuclear Ca^{2+} levels

Considering that the *cta4*$^+$ deletion mutant displayed a Ca^{2+}-sensitive phenotype, it was tempting to speculate that Cta4 ATPase would play a role in controlling cytosolic-free calcium levels. To test this possibility, we explored the FRET-based technique using "*cameleon*" reporter constructs expressed in living cells to measure Ca^{2+} levels by time-lapse yellow fluorescent protein (YFP)/cyan fluorescent protein (CFP) ratio imaging (Miyawaki et al., 1997). The cameleon reporter consists of a CFP-M13-CaM-YFP protein fusion, which gives a relative increase in YFP emission (at 535 nm) when Ca^{2+} levels are high. This is due to FRET from CFP to YFP caused by proximity of CFP and YFP when M13 interacts with Ca^{2+}-bound CaM. The yellow cameleon YC2 was cloned into pREP3x plasmid (see Materials and methods), and the resulting plasmid was introduced into wild-type *S. pombe* cells and cells lacking *cta4*$^+$ by transformation. To increase the signal for accurate determination of the FRET signal, a nuclear localization signal was added to the YC2 protein fusion and strong expression (thiamine) was used from the pREP3x *nmt1*$^+$ promoter. The ratio imaging measurements indicated that the ratio of 535:480 fluorescence increased significantly ($t = 4.125$, $P < 0.001$) in untreated *cta4Δ* cells compared with wild-type cells and in *cta4Δ* cells treated with Ca^{2+} compared with wild-type cells treated with Ca^{2+} ($t = 3.154$, $P = 0.003$). The 535:480 ratio in Ca^{2+}-treated *cta4Δ* cells was on average 1.59 ($n = 21$), whereas Ca^{2+}-treated wild-type cells gave 535:480 ratios on average of 1.39 ($n = 18$). The 535:480 ratios were generally stable over time. It was noticed that all aberrantly shaped or round *cta4Δ* cells examined gave particularly high FRET 535:480 ratios on average of 1.78 ($n = 15$): for example, the cell nucleus indicated in red in Fig. 8 C. Thus, the cell shape defects caused by loss of *cta4*$^+$ are associated with elevated nuclear Ca^{2+} level.

Discussion

In the present work, we undertook a genetic approach to gain insight into the role of a putative P-type ATPase in fission yeast. Cta4 ATPase belongs to a P4 subfamily of the P-type ATPases with an unknown substrate specificity and subcellular localization (Catty et al., 1997). This recently identified subfamily comprises, in addition to *cta4*$^+$, *SPF1* and Yor291 of *S. cerevisiae* and several homologous genes found in the genomes of *Plasmodium*, *Caenorhabditis*, *Tetrahymena*, and Arabidopsis

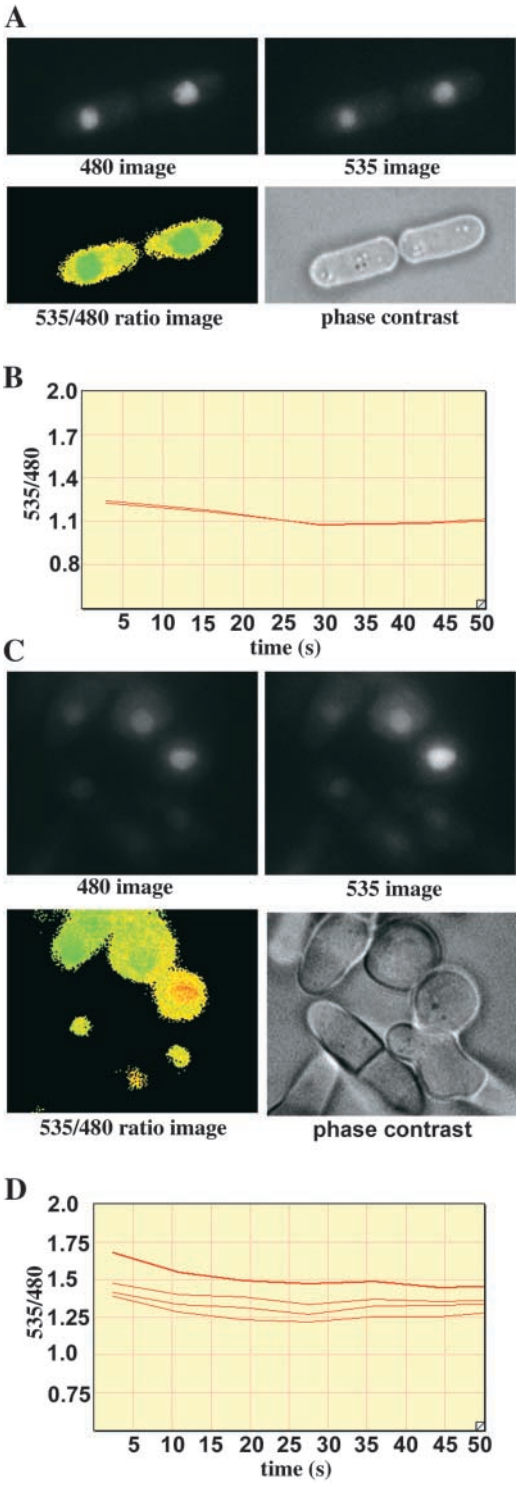

Figure 8. **Measurement of $[Ca^{2+}]_{nuc}$ in live fission yeast cells using yellow cameleon YC.2.** (A and C) Images of wild-type (A) and *cta4Δ* (C) cells. Yeast cells expressing the yellow cameleon pREP3x-YC2 plus NLS were grown at 30°C and treated with 100 mM $CaCl_2$ for 1 h and then subjected to ratio imaging. The raw data image of CFP (480 nm) and YFP (535 nm) emissions are shown. The 535:480 ratio image (bottom left) indicates the $[Ca^{2+}]_{nuc}$ using a "rainbow" scale in which green indicates low, yellow indicates intermediate, and red indicates high YFP to CFP ratios. (B and D) Time course analysis of the 535:480 emission ratios on the same yeast cells as in A and C. Wild-type (B) and *cta4Δ* (D) cells were subjected to time-lapse ratio imaging analysis at 30°C. The y axis shows the ratio of the YFP to CFP signal in the nuclei of the cells, which indicates $[Ca^{2+}]_{nuc}$. The x axis shows the real time in seconds.

(Catty et al., 1997; Suzuki and Shimma, 1999; Axelsen and Palmgren, 2001). Although amino acid homology between P4 ATPases could be as little as 20%, these pumps contain specific conserved amino acid signatures, suggesting that they might have common substrate and/or common mechanism of regulation and related cellular functions. The *cta4*$^+$ gene product is most closely related to the budding yeast ATPase Spf1. The function of Spf1p is little understood. It has been shown that *spf1* disruption leads to a resistance to *P. farinosa* killer toxin and impaired glycosylation (Suzuki and Shimma, 1999) and that Spf1/Cod1 regulates a degradation of integral ER membrane protein hydroxymethylglutaryl–coenzyme A (CoA) reductase (Cronin et al., 2000). Gene disruption experiments indicated that the *cta4*$^+$ gene was nonessential for viability. Yet the *cta4*-null mutant displayed pleiotropic cellular phenotypes. The cell growth was reduced at 25°C and arrested at 36°C. Loss of *cta4*$^+$ resulted in multiseptated hyphae-like structures in which cells did not separated and were often branched and aggregated. The microtubule structure was destabilized. Adaptation to cation stress was also impaired. Similarly to *spf1* null, *cta4Δ* cells were resistant to SMKT killer toxin. However, whether the *spf1* and *cta4* genes are functionally interchangeable remains to be determined. It is of note that contrary to *cta4Δ* cells, lack of Spf1 ATPase did not cause visible changes in ion homeostasis, since *spf1* growth was independent of calcium and manganese (Suzuki and Shimma, 1999). On the other hand, the addition of high $CaCl_2$ (200 mM) to extracellular medium could restore a defect in hydroxymethylglutaryl-CoA reductase degradation displayed by *spf1* cells (Cronin et al., 2000).

Several lines of evidence suggest that *cta4*$^+$ is involved in Ca^{2+} homeostasis. First, *cta4Δ* was unable to grow when calcium was supplied to medium and when it was chelated by EGTA (unpublished data). Second, calcium measurements in *cta4Δ* cells using fluorescent indicator yellow cameleon showed that nuclear calcium levels were increased in *cta4*-null cells in comparison with wild-type cells. It is likely that nuclear Ca^{2+} levels are indicative of the cytoplasmic Ca^{2+} levels, since Ca^{2+} ions can diffuse through the nuclear pores (Lipp et al., 1997). Thus, loss of *cta4*$^+$ function reduces the ability to sequester Ca^{2+} to internal stores, presumably the ER (see below). The consequence of this is an increase in intracellular Ca^{2+}.

The *cta4* mutant cells were sensitive to inhibition of calcineurin, Ca^{2+}/CaM-dependent protein phosphatase type 2B, by CsA. The *ppb1*$^+$ gene of *S. pombe* encodes a catalytic subunit of calcineurin. In this respect, it is noteworthy that pleiotropic phenotypes of *cta4Δ* were reminiscent of those reported previously for *ppb1Δ* mutants regarding growth characteristics, septation, cell shape defects, and microtubule integrity (Yoshida et al., 1994). Moreover, *S. pombe* mutants lacking *cta4*$^+$ were, like *S. cerevisiae* calcineurin mutants, sensitive to Ca^{2+} and Mn^{2+} cation stress. Thus, it is possible that calcineurin function is defective in *cta4*-null cells. It remains to be determined if the *cta4*$^+$ and *ppb1*$^+$ genes interact and if these two gene products share an essential overlapping function. Finally, *cta4*$^+$ overexpression was toxic to wild-type cells, and

this could be overcome by addition of Ca^{2+} (unpublished data). Therefore, both elevated and lowered Ca^{2+} cytosolic levels may be deleterious to *S. pombe.* Since *cta4*$^{+}$ deletion is not lethal to *S. pombe* cells, it could be concluded that other Ca^{2+} transporters deplete cytosolic Ca^{2+} in this genetic background, although to a lesser extent than *cta4*$^{+}$ normally does. Therefore, the precise regulation of Ca^{2+} homeostasis fails and, consequently, Ca^{2+} signals.

From our results it could be presumed that Cta4p might transport Ca^{2+}. However, direct biochemical evidence is needed to establish the exact substrate specificity of Cta4p. Our attempts to measure ATP-dependent Ca^{2+} transport in isolated membranes of *S. pombe* 972 have shown that all Ca^{2+} uptake was abolished by protonophore FCCP, indicating that Ca^{2+} transport was due to Ca^{2+}/H^{+} exchange (Okorokov et al., 2001). The similar result was obtained with *S. pombe* strain Hu237 used for determination of subcellular localization of Cta4p (unpublished data). Further experiments will be necessary to find the conditions favoring a detection of biochemical activity of Cta4 ATPase. The biochemical characterization of Cta4p will contribute to our comprehension of the physiological function of P4 ATPases.

Cta4p localizes to the ER in *S. pombe*. In animal cells, ER is equipped with SERCA-type Ca^{2+}-ATPase and is a main Ca^{2+} store compartment (Mendolesi and Pozzan, 1998; Carafoli and Brini, 2000). The ATPases belonging to SERCA-type were also found in plant, protozoa, and insect (Liang et al., 1997; Lockyer et al., 1998; Talla et al., 1998). Interestingly, the gene encoding for SERCA-type Ca^{2+} pump has not been identified in yeast, although Ca^{2+}-ATPase activity could be detected in the *S. cerevisiae* membranes derived from the ER (Okorokov and Lehle, 1998; unpublished data). These observations raise a possibility that Cta4p could represent a primary ancient pump serving the ER. It is likely that the evolution of the ER as an organelle was driven by a wide range of functions supporting the development of complex signaling networks within the eukaryotic cell. This may have been the driving force leading to the appearance of additional specialized ATPases, such as SERCA, which may sequester calcium ions into the ER.

The pleiotropic defects exhibited by *cta4Δ* could be interpreted by either a direct or an indirect involvement of *cta4*$^{+}$ in microtubule integrity, cell shape, and cytokinesis through regulated changes in Ca^{2+} concentrations. Since Ca^{2+} is a well-known secondary messenger, any transient elevations in the intracellular Ca^{2+} concentration would result in Ca^{2+} binding to multiple classes of Ca^{2+}-binding proteins, each of which can, in its turn, regulate multiple downstream signaling pathways. On the other hand, Ca^{2+} is emerging as the regulatory ion for many ER/Golgi functions. Oscillations in free Ca^{2+} concentrations in the ER of animal cells were shown to control diverse processes, including protein synthesis, chaperone function, and glycoprotein processing (Corbett and Michalak, 2000). The budding yeast secretory pathway requires Ca^{2+} for proper glycosylation, sorting, and ER-associated protein degradation (Antebi and Fink, 1992; Durr et al., 1998; Okorokov and Lehle, 1998). Further studies are required to identify components of the Ca^{2+} signaling machinery, which depend on Cta4p. However, some speculations about possible downstream targets can be made already.

We showed that loss of *cta4*$^{+}$ enables yeast cells to complete cytokinesis. Previously, this process was shown to be dependent, in part, on the *cps1*$^{+}$ gene encoding β-(1,3)-D-glucan synthase (Ishiguro et al., 1997; Liu et al., 2000). Expression of a homologue of *cps1*$^{+}$ in budding yeast, *FKS2*, is induced by PKC together with calcineurin in a Ca^{2+}-dependent manner (Zhao et al., 1998). *cps1*$^{+}$ also appears to be dependent on calcineurin, since the *cps1*^{ts} mutant is hypersensitive to CsA (Ishiguro et al., 1997). In addition, *cps1*^{ts} mutants are, like *cta4Δ*, multiseptated and branched. Considering our supposition that calcineurin function might be compromised in *cta4Δ*, then defects in cytokinesis could be explained through changes in Cps1 activity, and this raises the possibility that *cta4*$^{+}$ and *cps1*$^{+}$ act in the same pathway.

There is a strong link between cell shape/polarity and microtubules in fission yeast (Sawin and Nurse, 1998). Therefore, our data provide evidence that microtubule integrity relies on *cta4*$^{+}$ function. From this study, we cannot distinguish direct from indirect effects of Ca^{2+} on microtubules. Thus, additional studies will be necessary to gain a deeper comprehension of the involvement of *cta4*$^{+}$ in this process. One of the possibilities is that *cta4*$^{+}$ would regulate microtubule integrity, controlling the stability and/or deposition of microtubule-associated proteins. A recent study in animal cells has shown that Ca^{2+}-binding proteins, such as S100A1 and S100B, might have a role in the in vivo regulation of the state of assembly of microtubules in a Ca^{2+}-regulated manner (Sorci et al., 2000). Also, in *S. pombe*, microtubule-associated factors, such as the CLIP170-like protein Tip1, are involved in microtubule dynamics (Brunner and Nurse, 2000). The phenotypes of *tip1Δ* null and *cta4Δ* are related, since the mutants cells are not rod-shaped like wild-type *S. pombe* cells. Furthermore, both mutants show shorter microtubules and an increase in the frequency of microtubule catastrophe events throughout the cell rather than exclusively in the cell tips, which are the regions of polarized growth (Fig. 7) (Brunner and Nurse, 2000). In both cases, the changes in cell shape are associated with a defective guidance mechanism for microtubules. In this respect, since Tip1p is a microtubule-binding protein it would be interesting to investigate if Tip1p is directly or indirectly dependent on Ca^{2+} and/or Cta4p.

We provide evidence that the Ca^{2+} concentration is crucial for establishing the correct cell polarity by regulating microtubule dynamics. This finding is not without precedence, since studies in plant root tips demonstrate that root hair polarity is dependent on a Ca^{2+} gradient that increases in Ca^{2+} concentration toward the tip of the root hair (Bibikova et al., 1997; Wymer et al., 1997; Gadella et al., 1999). Furthermore, the polarity marked by this gradient is dependent on microtubules (Bibikova et al., 1999). Thus, the Ca^{2+}-dependent mechanisms operating with respect to cell polarity may likely be of general significance in eukaryotes.

Further measurements of cytosolic Ca^{2+} are needed to clarify whether a Ca^{2+} gradient exists within the yeast cell and if there is a correlation between localized high Ca^{2+} and the sites of polarized growth. At the moment, it is tempting to speculate that increased Ca^{2+} at the ends of the cells would be a guiding signal for microtubule growth and a factor that induces the occurrence of microtubule catastrophe events.

Table III. **Yeast strains used in this study**

Strain	Genotype	Source
S. pombe		
972	*h*$^-$	
Fy1180	*h*$^+$ *otr1R(SphI)::ade6*$^+$ *ura4-D18 leu1-32 ade6-M210*	R. Allshire[a]
Hu185	*h*$^+$ *cta4-GFP::kanMX6 otr1R(SphI)::ade6*$^+$ *ura4-D18 leu1-32 ade6-M210*	This study
Hu285	*h*$^-$ *cta4:: ura4*$^+$ *ura4-D18 leu1-32 ade6-M216*	This study
Fy2796	*h*$^-$ *cta4:: ura4*$^+$ *ura4-D18 leu1-32 ade6-M210*	This study
Fy2773	*h*$^-$ *leu1-32 ura4-D18 ade6-M210 ars1::nmt1-a-Tub-GFP-LEU2+*	A. Pidoux[a]
Hu326	*h*$^-$ *cta4:: ura4*$^+$ *ura4-D18 leu1-32 ade6-M210 ars1::nmt1-α-Tub-GFP-LEU2+*	This study
Hu237	*cta4-GFP::kanMX6 otr1R(SphI)::ade6*$^+$ *ura4-D18 leu1-32 ade6-M210 pREP- nmt1-Sec61-myc-LEU2+*	This study
S. cerevisiae		
CS202A	*MATa his3Δ1 leu2-3 ura3-52 trp1-289 spf1::LEU2*	Suzuki and Shimma, 1999
CS202B	*MATa his3Δ1 leu2-3 ura3-52 trp1-289*	Suzuki and Shimma, 1999

[a]University of Edinburgh, Edinburgh, UK.

Materials and methods

Strains and media

Media used were prepared according to standard methods (Moreno et al., 1991). Strains used in this study are listed in Table III.

IF microscopy

S. pombe cells were prepared for IF microscopy according to the formaldehyde fixation procedure with some modifications (Hagan and Ayscough, 2000). Log phase cultures were incubated for 5–30 min in YES plus 1.2 M sorbitol before harvest. In most cases PEMAL (PEM plus 5 or 0.03% milk, 0.1 M L-lysine HCl, cleared by centrifugation during 30 min at 20,000 *g*) was used instead of PEMBAL. As primary antibodies, rabbit anti-GFP (Molecular Probes), mouse anti-myc (Sigma-Aldrich), and rabbit anti-BiP (Pidoux and Armstrong 1993) were used. FITC- or Texas red–conjugated secondary antibodies were purchased from Jackson ImmunoResearch Laboratories or Sigma-Aldrich. Cells were visualized using a ZEISS Axioskop II imaging microscope equipped with a Hamamatsu C4742–95 CCD camera. Z-series digital confocal deconvolution analysis using Openlab software (version 2:25; Improvision), was performed using 0.2–0.3-μm sample z spacing and nearest neighbor deconvolution method. An object magnification of 100× and a lens aperture of 1.4 were used.

Live analysis of *S. pombe* cells

We performed GFP and CFP/YFP time-lapse analysis using the ratio imaging module of Openlab software version 2.25 and a ZEISS Axioskop II imaging microscope equipped with a Hamamatsu C4742–95 CCD camera. The yeast cells were embedded in 10 μl 1% soft agar in PMG medium under a 22 × 22-mm no. 1 coverslip (Propper) and subjected to time-lapse video capture using a 10% neutral density filter to reduce photobleaching of the GFP.

Membrane fractionation

Yeast cells were grown to late log phase. After incubation in 1.2 M sorbitol and 30 mM mercaptoethanol, pH 8.5, for 10 min at 25°C, they were washed with 1.2 M sorbitol and 50 mM NaH_2PO_4 adjusted with citric acid to pH 5.8. Spheroplasts were then isolated by incubation of the cells with lytic enzymes from *Tritrichoderma* at 30°C in the same buffer. Spheroplasts lysis and isolation of membranes followed published procedures (Okorokov and Lehle, 1998). The resuspended total membranes were loaded onto a step gradient formed of 56, 52, 48, 45, 42, 39, 36, 33, 30, and 25% sucrose (wt/wt). After centrifugation at 140,000 *g* for 2 h 45 min, the membrane fractions were collected from the bottom and stored at −70°C.

Immunoblotting

Yeast membranes from the sucrose gradient fractions (10 μl) were spotted on nitrocellulose membrane and probed with antibodies. Anti-GFP and anti-myc antibodies were purchased from Molecular Probes and Sigma-Aldrich, respectively. Anti-BiP antibodies were provided by Prof. J. Armstrong (University of Sussex, Brighton, UK). The blots were developed with peroxidase-conjugated secondary antibody.

Recombinant DNA

All procedures with recombinant DNA were performed according to standard techniques (Maniatis et al., 1982). The YC2 construct was PCR amplified from the original DNA clone (Miyawaki et al., 1997) using oligonucleotides that add a PKKKRKV (SV40) nuclear localization signal fused to the YC2 NH_2 terminus and cloned into pREP3× multicopy plasmid digested with SalI. The expression of *cta4*$^+$ was induced in PMG medium lacking thiamine. The *cta4*$^+$ gene was tagged at its endogenous site with GFP using the method from Bahler et al. (1998).

We thank A. Mutvei for comments on the article, C. Retamal for help with immunomeasurements, K. Cunningham and S. Suzuki for *S. cerevisiae* strains, C. Stirling for Sec61-myc, S. Suzuki for SMKT toxin, K. Gull for the Tat1 antibody, J. Armstrong for BiP antibody, A. Pidoux for the Fy2773 strain, and R. Tsien for cameleon pYC2.

This work was supported by the Swedish Medical Research Council VR-M grant no. 12562 to K. Ekwall, Fundação Carlos Chagas Filho de Amparo à Pesquisa do Estado do Rio de Janeiro grant E-26/171.374/99 to L. Okorokova, a Natural Science Council VR-N open postdoc grant to H. Appelgran, and a Wennergren stipend to M. Tabish.

Submitted: 5 November 2001
Revised: 28 February 2002
Accepted: 3 April 2002

References

Antebi, A., and G.R. Fink. 1992. The yeast Ca^{2+}-ATPase homologue, PMR1, is required for normal Golgi function and localizes in a novel-like distribution. *Mol. Biol. Cell.* 3:633–654.

Axelsen, K.B., and M.G. Palmgren. 2001. Inventory of the superfamily of P-type ion pumps in Arabidopsis. *Plant Physiol.* 126:696–706.

Bahler, J., J.Q. Wu, M.S. Longtine, N.G. Shah, A. McKenzie III, A.B. Steever, A. Wach, P. Philippsen, and J.R. Pringle. 1998. Heterologous modules for efficient and versatile PCR-based gene targeting in *Schizosaccharomyces pombe. Yeast.* 14:943–951.

Bibikova, T.N., A. Zhigilei, and S. Gilroy. 1997. Root hair growth is directed by calcium and endogeneous polarity. *Planta.* 203:495–505.

Bibikova, T.N., E.B. Blancaflor, and S. Gilroy. 1999. Microtubules regulate tip growth and orientation in root hairs of *Arabidopsis thaliana. Plant J.* 17:657–665.

Broughton, J., D. Swennen, B.M. Wilkinson, P. Joye, C. Gaillardin, and C.J. Stirling. 1997. Cloning of SEC61 homologues from *Schizosaccharomyces pombe* and *Yarrowia lipolytica* reveals the extent of functional conservation within this core component of the ER translocation machinery. *J. Cell Sci.* 110:2715–2727.

Brunner, D., and P. Nurse. 2000. CLIP170-like tip1p spatially organizes microtubular dynamics in fission yeast. *Cell.* 102:695–704.

Carafoli, E., and M. Brini. 2000. Calcium pumps: structural basis for and mechanism of calcium transmembrane transport. *Curr. Opin. Chem. Biol.* 4:152–161.

Catty, P., A. de Kerchove d'Exaerde, and A. Goffeau. 1997. The complete inventory of the yeast *Saccharomyces cerevisiae* P-type transport ATPases. *FEBS Lett.* 409:325–332.

Clapham, D.E. 1995. Calcium signaling. *Cell.* 80:259–268.

Corbett, E.F., and M. Michalak. 2000. Calcium, a signaling molecule in the endoplasmic reticulum? *Trends Biochem. Sci.* 25:307–311.

Cronin, S.R., A. Khoury, D.K. Ferry, and R.Y. Hampton. 2000. Regulation of HMG-CoA reductase degradation requires the P-Type ATPase Cod1p/

Spf1p. *J. Cell Biol.* 148:915–924.

Cunningham, K.W., and G.R. Fink. 1996. Calcineurin inhibits *VCX*1-dependent H^+/Ca^{2+} exchange and induces Ca^{2+} ATPases in *Saccharomyces cerevisiae. Mol. Cell. Biol.* 16:2226–2237.

Ding, D.-Q., Y. Chikashige, T. Haraguchi, and Y. Hiraoka. 1998. Oscillatory nuclear movement in fission yeast meiotic prophase is driven by astral microtubules, as revealed by continuous observation of chromosomes and microtubules in living cells. *J. Cell Sci.* 111:701–712.

Durr, G., J. Strayle, R. Plemper, S. Elbs, S.K. Klee, P. Catty, D.H. Wolf, and H.K. Rudolph. 1998. The medial-Golgi ion pump Pmr1 supplies the yeast secretory pathway with Ca^{2+} and Mn^{2+} required for glycosylation, sorting, and endoplasmic reticulum-associated protein degradation. *Mol. Biol. Cell.* 9:1149–1162.

Gadella, T.W.J., G.N.M. van der Krogt, Jr., and T. Bisseling. 1999. GFP-based FRET microscopy in living plant cells. *Trends Plant Sci.* 4:287–291.

Ghislain, M., A. Goffeau, D. Halachmi, and Y. Eilam. 1990. Calcium homeostasis and transport are affected by disruption of cta3, a novel gene encoding Ca^{2+}-ATPase in *Schizosaccharomyces pombe. J. Biol. Chem.* 265:18400–18407.

Greenfield, J.J., and S. High. 1999. The Sec61 complex is located in both the ER and the ER-Golgi intermediate compartment. *J. Cell Sci.* 112:1477–1486.

Guerini, D., and E. Carafoli. 1999. The calcium pumps. *In* Calcium as a Cellular Regulator. E. Carafoli and C.B. Klee, editors. Oxford University Press, Oxford, UK. 249–278.

Gunteski-Hamblin, A.-M., D.M. Clarke, and G.E. Shull. 1992. Molecular cloning and tissue distribution of alternatively spliced mRNAs encoding possible mammalian homologues of the yeast secretory pathway calcium pump. *Biochemistry.* 31:7600–7608.

Hagan, I.M., and K.R. Ayscough. 2000. Fluorescence microscopy in yeast. *In* Protein Localization by Fluorescence Microscopy. A Practical Approach. V.J. Allan, editor. Oxford University Press, Oxford. 179–206.

Ishiguro, J., A. Saitou, A. Durán, and J.C. Ribas. 1997. *cps1*$^+$, a *Schizosaccharomyces pombe* gene homolog of *Saccharomyces cerevisiae FKS* genes whose mutation confers hypersensitivity to Cyclosporin A and Papulacandin B. *J. Bacteriol.* 179:7653–7662.

Kamhi-Nesher, S., M. Shenkman, S. Tolchinsky, S.V. Fromm, R. Ehrlich, and G.Z. Lederkremer. 2001. A novel quality control compartment derived from the endoplasmic reticulum. *Mol. Biol. Cell.* 12:1711–1723.

Kaufman, R.J., M. Swaroop, and P. Murtha-Riel. 1994. Depletion of manganese within the secretory pathway inhibits O-linked glycosylation in mammalian cells. *Biochemistry.* 33:9813–9819.

Li, C.-J., R. Heim, P. Lu, Y. Pu, R.Y. Tsien, and D.C. Chang. 1999. Dynamic redistribution of calmodulin in HeLa cells during cell division as revealed by a GFP-calmodulin fusion protein technique. *J. Cell Sci.* 112:1567–1577.

Liang, F., K.W. Cunningham J.F. Harper, and H. Sze. 1997. ECA1 complements yeast mutants defective in Ca^{2+} pumps and encodes an endoplasmic reticulum-type Ca^{2+}-ATPase in *Arabidopsis thaliana*. *Proc. Natl. Acad. Sci. USA.* 94:8579–8584.

Lipp, P., D. Thomas, M.J. Berridge, and M.D. Bootman. 1997. Nuclear calcium signalling by individual cytoplasmic calcium puffs. *EMBO J.* 16:7166–7173.

Liu, J., H. Wang, and M.K. Balasubramanian. 2000. A checkpoint that monitors cytokinesis in *Schizosaccharomyces pombe. J. Cell Sci.* 113:1223–1230.

Lockyer, P.J., E. Puente, J. Windass, F. Earley, J.M. East, and A.G. Lee. 1998. Cloning and expression of an insect Ca^{2+}-ATPase from *Heliothis virescens. Biochim. Biophys. Acta.* 1369:14–18.

Maniatis, T., E.F. Fritsch, and J. Sambrook. 1982. Molecular Cloning: A Laboratory Manual. Cold Spring Harbor Laboratory Press, Cold Spring Harbor, NY. 545 pp.

Mendolesi, J., and T. Pozzan. 1998. The endoplasmic reticulum Ca^{2+} store: a view from the lumen. *Trends Biochem. Sci.* 23:10–14.

Mendoza, I., F.J. Quintero, R.A. Bressan, P.M. Hasegawa, and J.M. Pardo. 1996. Activated calcineurin confers high tolerance to ion stress and alters the budding pattern and cell morphology of yeast cells. *J. Biol. Chem.* 271:23061–23067.

Miyawaki, A., J. Llopis, R. Heim, J.M. McCaffery, J.A. Adams, M. Ikura, and R.Y. Tsien. 1997. Fluorescent indicators for Ca^{2+} based on green fluorescent proteins and calmodulin. *Nature.* 388:882–887.

Moreno, S., A. Klar, and P. Nurse. 1991. Molecular genetic analysis of fission yeast *Schizosaccharomyces pombe. Methods Enzymol.* 194:795–823.

Moser, M.J., M.R. Flory, and T.N. Davis. 1997. Calmodulin localizes to the spindle pole body of *Schizosaccharomyces pombe* and performs an essential function in chromosome segregation. *J. Cell Sci.* 110:1805–1812.

Nagase, T., M. Nakayama, D. Nakajima, R. Kikuno, and O. Ohara. 2001. Prediction of the coding sequences of unidentified human genes. XIX. The complete sequences of 100 new cDNA clones from brain which code for large proteins in vitro. *DNA Res.* 8:85–95.

Nakamura, T., Y. Liu, D. Hirata, H. Namba, S. Harada, T. Hirokawa, and T. Miyakawa. 1993. Protein phosphatase type 2B (calcineurin)-mediated, FK506-sensitive regulation of intracellular ions in yeast as an important determinant to high salt stress conditions. *EMBO J.* 12:4063–4071.

Nishikawa, T., H. Aiba, and T. Mizuno. 1999. The *cta3*$^+$ gene that encodes a cation-transporting P-type ATPase is induced by salt stress under control of the Wis1-Sty1 MAPKK-MAPK cascade in fission yeast. *FEBS Lett.* 455:183–187.

Okorokov, A.L., and L. Lehle. 1998. Ca^{2+}-ATPases of *Saccharomyces cerevisiae*: diversity and possible role in protein sorting. *FEMS Microbiol. Lett.* 162:83–91.

Okorokov, L.A., F.E. Silva, and A.L. Okorokova Facanha. 2001. Ca^{2+} and H^+ homeostasis in fission yeast: a role of Ca^{2+}/H^+ exchange and distinct V-H^+-ATPases of the secretory pathway organelles. *FEBS Lett.* 505:321–324.

Pedersen, P.L., and E. Carafoli. 1987a. Ion motive ATPases. I. Ubiquity, properties, and significance for cell function. *Trends Biochem. Sci.* 12:146–150.

Pedersen, P.L., and E. Carafoli. 1987b. Ion motive ATPases. II. Energy coupling and work output. *Trends Biochem. Sci.* 12:186–189.

Pidoux, A.L., and J. Armstrong. 1993. The BiP protein and the endoplasmic reticulum of *Schizosaccharomyces pombe*: fate of the nuclear envelope during cell division. *J. Cell Sci.* 105:1115–1120.

Pidoux, A.L., S. Uzawa, P.E. Perry, W.Z. Cande, and R.C. Allshire. 2000. Live analysis of lagging chromosomes during anaphase and their effect on spindle elongation rate in fission yeast. *J. Cell Sci.* 113:4177–4191.

Plochocka-Zulinska, D., G. Rasmussen, and C. Rasmussen. 1995. Regulation of calcineurin gene expression in *Schizosaccharomyces pombe. J. Biol. Chem.* 270:24794–24799.

Rudolph, H.K., A. Antebi, G.R. Fink, C.M. Buckley, T.E. Dorman, J. LeVitre, L.S. Davidow, J.I. Mao, and D.T. Moir. 1989. The yeast secretory pathway is perturbed by mutations in *PMR*1, a member of a Ca^{2+} ATPase family. *Cell.* 58:133–145.

Sanders, D., C. Brownlee, and J.F. Harper. 1999. Communication with calcium. *Plant Cell.* 11:691–706.

Sawin, K.E., and P. Nurse. 1998. Regulation of cell polarity by microtubules in fission yeast. *J. Cell Biol.* 142:457–471.

Sorci, G., A.L. Agnelett, and R. Donato. 2000. Effects of S100A1 and S100B on microtubule stability. An in vitro study using triton-cytoskeletons from astrocyte and myoblast cell lines. *Neuroscience.* 99:773–783.

Sorin, A., G. Rosas, and R. Rao. 1997. PMR1, a Ca^{2+}-ATPase in yeast Golgi, has properties distinct from sarco/endoplasmic reticulum and plasma membrane calcium pumps. *J. Biol. Chem.* 272:9895–9901.

Stull, J.T. 2001. Ca^{2+}-dependent cell signaling through calmodulin-activated protein phosphatase and protein kinase minireview series. *J. Biol. Chem.* 276: 2311–2312.

Suzuki, C., and Y. Shimma. 1999. P-type ATPase *spf1* mutants show a novel resistance mechanism for the killer toxin SMKT. *Mol. Microbiol.* 32:813–823.

Suzuki, C., Y. Ando, and S. Machida. 2001. Interaction of SMKT, a killer toxin produced by *Pichia farinosa*, with the yeast cell membranes. *Yeast.* 18:1471–1478.

Talla, E., R.L. de Mendonça, I. Degand, A. Goffeau, and M. Ghislain. 1998. *Schistosoma mansoni* Ca^{2+}-ATPase SMA2 restores viability to yeast Ca^{2+}-ATPase-deficient strains and functions in calcineurin-mediated Ca^{2+} tolerance. *J. Biol. Chem.* 273:27831–27840.

Wymer, C.L., T.N. Bibikova, and S. Gilroy. 1997. Cytoplasmic free calcium distributions during the development of root hairs of *Arabidopsis thaliana. Plant J.* 12:427–439.

Yoshida, T., T. Toda, and M. Yanagida. 1994. A calcineurin-like gene *ppb1*$^+$ in fission yeast: mutant defects in cytokinesis, cell polarity, mating and spindle pole body positioning. *J. Cell Sci.* 107:1725–1735.

Zhao, C., U.S. Jung, P. Garrett-Engele, T. Roe, M.S. Cyert, and D.E. Levin. 1998. Temperature-induced expression of yeast FKS2 is under the dual control of protein kinase C and calcineurin. *Mol. Cell Biol.* 18:1012–1022.